Solar-Terrestrial Physics. 2022. Vol. 8. Iss. 2. P. 84–90. DOI: 10.12737/stp-82202213. © 2022
A.V. Vorobev, A.A. Soloviev, V.A. Pilipenko, G.R. Vorobeva. Published by INFRA-M Academic Publishing House

UDC 53.05
DOI: 10.12737/stp-82202213

Received February 17, 2022
Accepted May 23, 2022

INTERACTIVE COMPUTER MODEL FOR AURORA FORECAST AND ANALYSIS

A.V. Vorobev
Geophysical Center RAS,
Moscow, Russia, geomagnet@list.ru
Ufa State Aviation Technical University,
Ufa, Russia

A.A. Soloviev
Geophysical Center RAS,
Moscow, Russia, a.soloviev@gcras.ru
Schmidt Institute of Physics of the Earth, RAS,
Moscow, Russia

V.A. Pilipenko
Geophysical Center RAS,
Moscow, Russia, pilipenko_va@mail.ru
Schmidt Institute of Physics of the Earth, RAS,
Moscow, Russia

G.R. Vorobeva
Ufa State Aviation Technical University,
Ufa, Russia, gulnara.vorobeva@gmail.com

Abstract. An interactive computer model of a short-term (with a horizon 30–70 min) forecast of aurora intensity has been developed in the form of a web-based geoinformation system. The OVATION-Prime empirical model is used as the basic software, which establishes statistical relationships between parameters of the solar wind, the interplanetary magnetic field, and auroral particle fluxes. On the basis of this model, a system has been built which simulates the spatial planetary distribution of the probability of observing auroras and a number of accompanying quantities. Data visualization is carried out on the basis of the virtual globe technology and is provided to the end user via a specialized web service. The forecast has been verified by comparing the model predictions with the data from 16 cameras conducting continuous observations of the auroras in the visible spectrum. The proportion of coincidences between the predicted and observed auroras was 86 %. The developed service enables both forecasting and analysis of past events. The system allows us to compare the spatial distribution of probability of auroras with railway transport systems for the territory of the Russian Federation.

Keywords: auroras, magnetic storms, auroral zone, space weather, geoinformation system.

INTRODUCTION

The greatest risks caused by the negative impact of space weather on the reliability of objects of Earth's technosphere such as overloads of electric power transmission lines [Pulkkinen et al., 2005; Sokolova et al., 2019; Pilipenko, 2021], failures of power distribution systems and automation of railways [Ptitsyna et al., 2008; Rozenberg, 2021] occur at high latitudes in the auroral oval zone representing a belt of intense auroras created by electron precipitation into the atmosphere from near-Earth space. Global Navigation Satellite Systems (GNSS) GPS and GLONASS [Afraimovich et al., 2009; Zakharov et al., 2020; Demyanov, Yasyukevich, 2021] also have problems with accuracy and fault tolerance. For example, it is in the auroral zone due to its characteristic sharp gradients, high level of turbulence of ionospheric plasma, and electrojets that frequent navigation signal phase slips and extreme positioning errors are recorded. As a consequence, in GPS receivers the high-precision navigation (PPP mode) error can increase up to five times relative to the background level in the region of auroral electron precipitation into the ionosphere [Yasyukevich, 2020]. During periods of high geomagnetic activity, the auroral oval descends to lower latitudes, and the area of reduced navigation signal detection quality extends to midlatitudes. Thus, the real-time forecast of the position of the auroral oval and the aurora intensity can improve the efficiency of decisions taken in the management of energy, infocommunication, transport, and navigation systems in high-latitude regions.

Several approaches to monitoring spatial and energy characteristics of the auroral oval have been proposed. The ionospheric electrojet and geomagnetic Pc5 pulsations are closely linked to the auroral oval, which makes it possible to track the position of the oval from ground-based geomagnetic data [Martines-Bedenko et al., 2018; Penskikh et al., 2021].

The most reliable models are thought to be the auroral oval models based on particle flux data from low-orbit satellites. The data does not depend on illumination of the ionosphere and cloudiness of the atmosphere, is available for both hemispheres, and is more sensitive to particle precipitation than ground or satellite optical observation data. A model predicting the planetary distribution of auroral particle precipitation of different types through statistical analysis of data from low-orbit DMSP (Defense Meteorological Satellite Program) satellites has been developed at PGI [Vorobjev, Yagodkina, 2005]. This model is, however, parametrized for the geomagnetic indices *AL* and *Dst*, so it cannot be used for prediction. The OVATION-

This is an open access article under the CC BY-NC-ND license

Prime (OP) model [Newell et al., 2014] based on 21 year (about two solar cycles) observations of electron and proton fluxes of different energies by DMSP satellites has received wide acceptance. This model is parameterized for the solar wind and the interplanetary magnetic field (IMF) parameters transmitted in real time from interplanetary satellites, which enables the real-time prediction of the auroral oval dynamics.

A web service supported by the US National Oceanic and Atmospheric Administration (NOAA) has been developed on the basis of the OP model [https://www.swpc.noaa.gov/products/aurora-30-minute-forecast]; it visualizes the short-term forecast of the planetary distribution of auroras. Also well-known are projects of the University of Alaska [https://www.gi.alaska.edu/monitors/aurora-forecast], the Meteorological Service of Iceland [https://en.vedur.is/weather/forecasts/aurora], etc., which are focused on regional monitoring of auroral oval fragments.

Study of the principles of operation and analysis of the architecture of the above and other similar software products has revealed a number of characteristic disadvantages of the web services repeated from implementation to implementation — lack of interactivity; inability to dynamically scale and add user interface layers; lack of basic tools for spatial analysis of visualized parameters; invariance of the set of visualized parameters, which significantly complicates the effective use of services of this kind.

Thus, developing and modernizing computer models that provide multiparametric forecast and visualization of auroral oval properties, as well as allow for their prompt geospatial analysis is a topical problem whose solution can promote a significant effect both in the fundamental research and in applications aimed at supporting decision-making in the management of complex technical objects in the Arctic region.

1. PHYSICAL PRINCIPLES OF MODEL DEVELOPMENT

As basic mathematical software we utilize the empirical OP model [Newell et al., 2009] that gets SW and IMF parameters as input. The model is based on the regression coefficients determined by season, aurora type, and a set of coordinates, including a total of 245760 regression relationships (4 seasons × 4 aurora types × 96 local time readings × 160 geomagnetic latitude readings). The local power of precipitation in the auroral zone p_A is calculated from the relation:

$$\begin{cases} p_A\left(\text{MLat, MLT, Q, G}\right) = a + b\left(\dfrac{d\Phi}{dt}\right) \\ \dfrac{d\Phi}{dt} = V^{4/3} B_T^{2/3} \sin^{8/3}\left(\dfrac{\theta}{2}\right) \end{cases}, \quad (1)$$

where $\text{MLat} \in \{[50...90] \cup [-50...-90]\}$ is the magnetic latitude with an increment of 0.25°; $\text{MLT} \in [0...24)$ is the magnetic local time with a sampling period of 0.25 hr; *a*, *b* are the regression coefficients determined by season Q and aurora type G for each MLat and MLT value [https://github.com/lkilco m mons/ OvationPyme];

$d\Phi/dt$ is the rate of change of the magnetic flux at the magnetopause, Wb/s; V is the solar wind velocity, km/s; B_y and B_z are IMF components, nT; $\theta=\arctan(B_y/B_z)$; $B_T = (B_y^2 + B_z^2)^{1/2}$ is the complete field transverse to the Earth—Sun line.

By combining auroras of four main types, we can obtain the spatial distribution of the total luminosity intensity

$$p_A\left(\text{MLat, MLT, } Q\right) = \sum_{g=1}^{G}\left[a_g + b_g\left(\frac{d\Phi}{dt}\right)\right]. \quad (2)$$

By summing up Expression (2) in longitude and latitude separately for each hemisphere, we can get an integral estimate of the aurora intensity in the Northern (N) and Southern (S) hemispheres [Newell et al., 2009]:

$$P_A^{(N,S)}\left(Q\right) = \sum_{g=1}^{G}\sum_{m=-90}^{90}\sum_{n=1}^{360}\left[a_{g,m,n} + b_{g,m,n}\left(\frac{d\Phi}{dt}\right)\right], \quad (3)$$

Thus, for $P_A \leq 20$ GW, there is a weak or visually indistinguishable aurora; at $20 \leq P_A \leq 50$, aurora can be seen only at a small distance from it; for $50 < P_A \leq 100$, aurora should be visible with unaided eye; $P_A > 100$ corresponds to extreme auroral activity and a significant expansion of the auroral oval to low latitudes.

The data required for the model on the parameters of the solar wind (V) and IMF (B_y, B_z), recorded by ACE and DSCOVR satellites at a distance of ~200 R_E from Earth, is provided in real time by services of the Space Weather Prediction Center (SWPC) [https://www.swpc.noaa.gov] and Goddard's Space Flight Center (GSFC) [https://omniweb.gsfc.nasa.gov]. The presence of history of these interplanetary medium parameters makes it possible to analyze the retrospective planetary distribution of auroras predicted by the OP model.

2. VISUALIZATION OF SIMULATION RESULTS

In general terms, at the output of model (2), the forecast of auroral oval characteristics as a visualization object is an array of spatial and attribute data whose processing and graphical interpretation are worth performing using web GIS technologies. The current experience of developing web-oriented GIS for visualization of geophysical parameters [Vorobyev et al., 2020a, 2020b, 2021] has shown that software and tools of this kind are well suited for addressing the tasks at hand.

According to the way spatial data is presented, modern GIS can be subdivided into classic flat charts and virtual globes. Taking into account the high-latitude nature of location of target objects, significant advantages of virtual globes are the quality of visual perception of the virtual model and the absence of cartographic distortions of projections typical of flat charts.

Thus, to solve the task at hand in the first approximation (without presenting requirements for the interface, input data format, tools supported by computer languages, etc.), we can use the entire gamut of cartographic libraries providing, at the web application level, work with data that has spatial binding and virtual globe visual-

ization mode (ArcGIS API, Cesium, Google Maps Platform, NASA World Wind, WebGLEarth, etc.). However, bearing in mind the possibility of using the Python-3 programming language, a set of spatial data processing methods adapted to the problems being solved, a wide community, and developed support, the subsystem for visualizing simulation results is proposed to build on the basis of ArcGIS API libraries [https://developers.arcgis.com/javascript/3]. Since the rate of rendering of simulation results is largely determined by resolution of loadable layers, and also taking into account the spatial resolution of the OP model in latitude (0.25°) and longitude (3.75°), it is assumed that in order to achieve this purpose we may restrict ourselves to small-scale basemaps with a scale from 1:2000000 to 1:10000000.

3. ARCHITECTURE OF INFORMATION SYSTEM

The proposed architecture of the software system (Figure 1) formalizing the computer model for aurora forecast is based on a combination of monolithic (traditional for web applications Web 2.0), microservice, and modular structures whose properties together provide high reactivity, flexibility, and extensibility of the application as a whole. We propose a three-level client-server architecture that ensures separation of data and business logic of the software system from its visualization for the end user. This approach minimizes the requirements for the hardware and software of the client side, practically reducing them to the presence of a device with a client agent (browser) and stable Internet access.

The program code is implemented in such a way that semantically similar computational processes are combined into separate software modules involving the operation of input and output information depending on the data processing problems to solve. The modular architecture of the program code not only made it possible to identify operations of the same type in the system, but also showed obvious advantages in the process of both functional and stress testing; and at the client side level, both visual testing and code refactoring during development. At the same time, semantic groups of software modules are considered as isolated layers.

In terms of the software system architecture described, functional modules are server-side; they provide reception, processing, analysis, and interpretation of spatial data. Moreover, they provide local database distribution and background (based on Cron principles) jobs of programming processes for interacting with external data sources. External data providers can give their own API that implements an “entry point” to the relevant data, as well as provide third-party users and applications with access via one of the network protocols (usually FTP). In the context of implementing data interaction at the level of the web application considered, both approaches are allowed, each providing data needed for processing, analysis, and interpretation. It is important to note the heterogeneity of the spatial data sources involved in the information support of the application (formats, sampling period, qualitative composition of data, etc.). Interaction with external data sources is on the server side to ensure the security of the application and prevent collisions caused by the cross-origin resource sharing (CORS).

The main application business logic is concentrated in a group of software modules conventionally called a processing layer (see Figure 1). Its input receives spatial information from local and external data sources from the data layer, and the result formed due to the operation of the modules is a spatial data set organized in JSON (GeoJSON), which is sent for subsequent rendering to the client side.

The modules in the processing layer consistently gain control of the corresponding information flow, and also provide for its processing, using client request para-

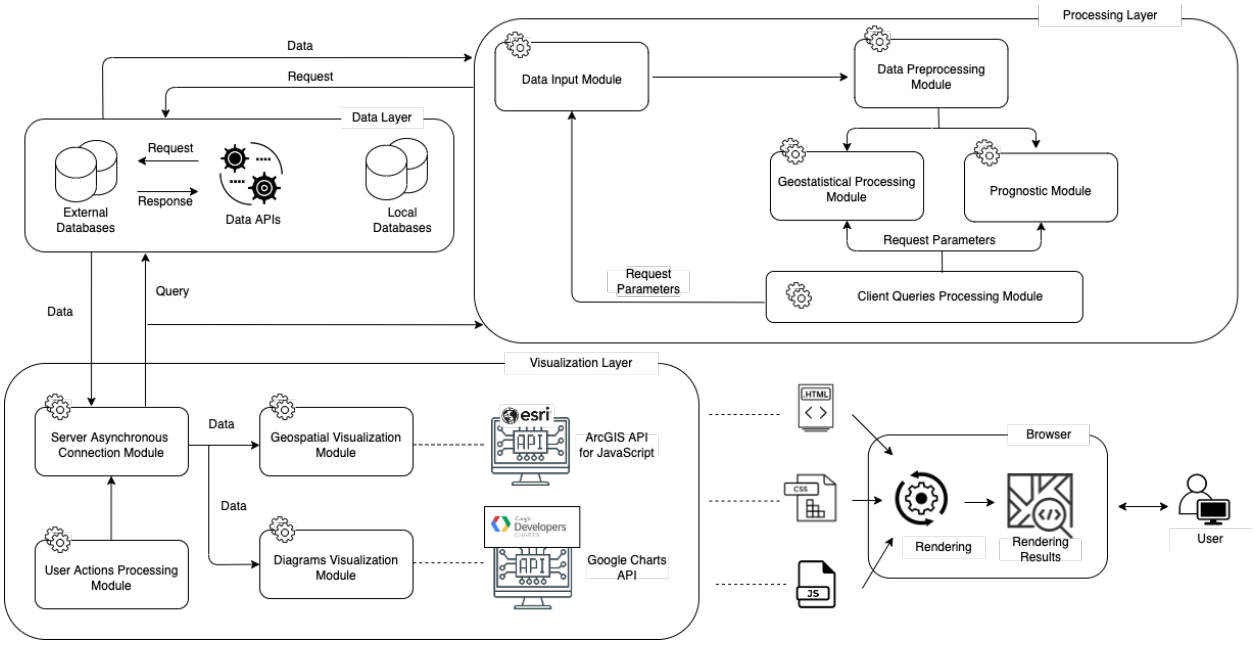

Figure 1. Information system architecture

meters (elements of horizontal/vertical data filtering, requested processing and/or analysis, etc. can be taken into account here). In this case, one entry point for the layer is a module that ensures data acquisition from sources of the data (see Figure 1). Operation of this module results in a virtual temporary storage, where information arrays received from data sources are placed for subsequent processing. A paired entry point to the layer is a module that provides processing of the request coming from the client side. During its operation, a set of parameters with corresponding values is extracted from the received request, which, in turn, determine the access to data sources, as well as processing and analysis procedures.

Since we deal with heterogeneous data sources, the data array formed by the previous software module is transmitted to the preprocessing module. Functionality of the module considered involves bringing the processed data to a general form (normalization), as well as removing obstacles to the subsequent processing (searching for gaps and interference in the data). Further, depending on the request received from the client side, we make a forecast and statistical processing of the relevant spatial data. As a result of the operation of the corresponding software module, an output spatial data flow presented in JSON (GeoJSON) format is formed; it is transmitted to the client side of the application. In terms of the software implementation, the architecture considered relies on the patterns of the Django framework (Model—View—Controller), which is due to the use of the Python-3 language on the server side.

The client part of the web application has a modular structure. In general, such software modules may be classified into two groups: one of them is responsible for processing the actions performed by a user in the application, and the other is responsible for the graphical representation, visualized during the corresponding rendering, of the spatial data processed on the server. The user actions that form a query to data sources are processed by the module of the same name and then transmit the corresponding parameters to the software module for interaction with the server. The latter, in turn, interacts with the server asynchronously, allowing a user to perform actions in the application while waiting for a response from the server. It also manages instances of software objects, which provide a connection to the web server, forward requests to it, using the GET method; as well as processes incoming responses. The spatial data sets generated by the server are received by the program object and transmitted to the visualization module. The proposed model is formalized as a web-based service available at [http://aurora-forecast.ru].

To assess the quality of the developed information system implementing the computer model for short-term forecast of auroras in the visible spectrum, we made load testing providing an assessment of web application performance and fault tolerance. The experimental studies were carried out on the client side, using a computer CPU Intel Core i5 10300H GHz (RAM 4 GB, Internet speed ~52.4 Mbit/s), and on the server side, using a web server with a processor 72* Intel(R) Xeon(R) Gold 6140 CPU @ 2.30 GHz. The maximum software system performance with this configuration was 15 connections (4816 processed requests) per hour. A long 24-hour fault tolerance testing revealed instability of the web application after switching off half of the server-cluster computers, which in the future can be compensated by horizontal scaling of hardware components of the system.

Morphological properties of model auroras

To roughly estimate plausibility of the OP model, we have used it to calculate a number of morphological characteristics of auroras. The computer model can digitally display different characteristics of model auroras, which a user can then analyze using various methods. Figure 2, *a* illustrates the seasonal variation in the median value of the parameter P_{A}^{N}, derived from Expression (3) for November 2020 – October 2021 (similar variation of the parameter P_{A}^{S}, for the Southern Hemisphere is almost identical). According to the results, P_{A}^{N} has a pronounced seasonal dependence with maxima in spring and fall (Figure 2, a). This dependence is consistent with the well-known seasonal distribution of auroras [Khorosheva, 1967].

Knowing the statistical distribution of the characteristic of the natural phenomenon makes it possible to estimate the probability of its extreme values. Figure 2, *b* presents the statistics of the forecast of the integrated value of P_{A} for the Northern Hemisphere for the period under study (the statistics of P_{A} for the Southern Hemisphere is similar). The resulting distribution $P_{\text{A}}^{N} \equiv P$ corresponds to exponential law (6),

$$PDF(P) = \exp(-P), \tag{6}$$

where PDF is a probability density function. With an increase in substorm activity, the distribution of P becomes lognormal (Figure 2, *c*):

$$PDF(P, s) = \frac{1}{sP\sqrt{2\pi}} \exp\left(-\frac{\log^2 P)}{2s^2}\right), \tag{7}$$

where s is the shape parameter. The lognormal distribution law is characteristic of magnetospheric-ionospheric phenomena. For example, Hardy et al. [2008] have analyzed the electron spectra recorded by nine DMSP satellites. The analysis of this extensive data archive showed that the distributions of energy flows corresponded either to lognormal law (7) or to a superposition of several lognormal distributions.

Thus, according to Figure 2, *b*, for solar minimum the average annual probability of observing auroras can be estimated as ~2.4 % $\left(P_{\text{A}}^{\text{N}} \geq 50\ \text{ГВт}\right)$, whereas the probability of observing extreme auroras is ~0.1 % $\left(P_{\text{A}}^{\text{N}} \geq 100\ \text{ГВт}\right)$.

4. VERIFICATION OF COMPUTER SIMULATION RESULTS

The computer model has been verified by comparing the predicted spatial distribution of auroras with observations by all-sky cameras at high latitudes (Table 1). For such a mass viewing of the presence or absence of auroras in 16 points, we used the citizen science approach [Kosar et al., 2018]. A group of researchers have analyzed images from cameras and recorded the presence/absence of auroras, entering data into the corresponding truth table (Table 2). This table indicates whether the model predict the occurrence of auroras for a given observation point correctly or not.

Table 1

All-sky cameras used to verify the computer model

№	Coordintes, °		Name	URL
	N	E		
1	78.15	16.04	Svalbard, Norway	https://aurorainfo.eu/aurora-live-cameras/svalbard-norway-all-sky-aurora-live-camera.jpg
2	69.35	19.13	Ramfjordmoen, Norway	https://aurorainfo.eu/aurora-live-cameras/ramfjordmoen-norway-all-sky-aurora-live-camera.jpg
3	69.02	20.85	Kilpisjarvi, Finland	https://aurorainfo.eu/aurora-live-cameras/kilpissafarit-all-sky-aurora-live-camera.jpg
4	67.85	20.41	Kiruna, Sweden	https://aurorainfo.eu/aurora-live-cameras/kiruna-sweden-all-sky-aurora-live-camera.jpg?1634790312
5	67.41	26.60	Sodankyla, Finland	https://aurorainfo.eu/aurora-live-cameras/sodankyla-finland-all-sky-aurora-live-camera.jpg
6	66.95	19.82	Porjus, Sweden	https://aurorainfo.eu/aurora-live-cameras/porjus-sweden-west-view-aurora-live-camera.jpg
7	66.58	18.85	Jokkmokk, Sweden	https://jokkmokk.jp/photo/nr3/latest.jpg
8	66.00	76.00	Novy Urengoy, Russia	https://starvisor.ru/wp-content/uploads/webcam/capture_nur.jpg
9	64.75	–147.3	North Pole, Alaska	https://auroranotify.com/image10.jpg
10	63.07	–151.00	Denali, Alaska	http://denaliview1.ddns.net:8080/nph-jpeg.cgi
11	62.39	26.43	Hankasalmi, Finland	https://aurorasnow.fmi.fi/public_service/images/latest_SIR_AllSky.jpg
12	62.30	–145.27	Gakona, Alaska	http://optics.gi.alaska.edu/realtime/latest/gak_latest.jpg
13	62.25	26.59	Hankasalmi, Finland	https://aurorainfo.eu/aurora-live-cameras/hankasalmi-finland-all-sky-aurora-live-camera.jpg
14	61.58	–147.45	Wasilla, Alaska	https://auroranotify.com/kickaxcamimage.jpg
15	61.52	23.50	Tampere, Finland	https://aurorainfo.eu/aurora-live-cameras/tampere-finland-aurora-live-camera.jpg
16	61.00	77.00	Strezhevoy, Russia	https://starvisor.ru/wp-content/uploads/webcam/185/capture.jpg

Table 2

Truth table for evaluating the computer model

Forecast of auroras	Actual observation of auroras	
	observed	not observed
Positive	A	B
Negative	C	D

Note:
A — the number of cases when the forecast was positive and aurora was observed
B — the number of cases when the forecast was positive, but no aurora was observed
C — the number of cases when the forecast was negative, but aurora was observed
D — the number of cases when the forecast was negative and no aurora was observed

5. USING THE MODEL FOR PREDICTING THE RISK TO INDUSTRIAL SYSTEMS FROM SPACE WEATHER DISTURBANCES

One of the features of the computer system developed is its caability of comparing spatial distributions of the auroral oval and various complex spatially distributed technological systems. Figure 3 presents the result of simulation of the spatial distribution of the parameter p_A, reduced to the probability of observing auroras for the substorm occurring on February 4, 2022 at 18:30 UT (*AE*~1480 nT). The green-yellow gradient of the isolines defines geographical boundaries of the region within which the probability of observing auroras

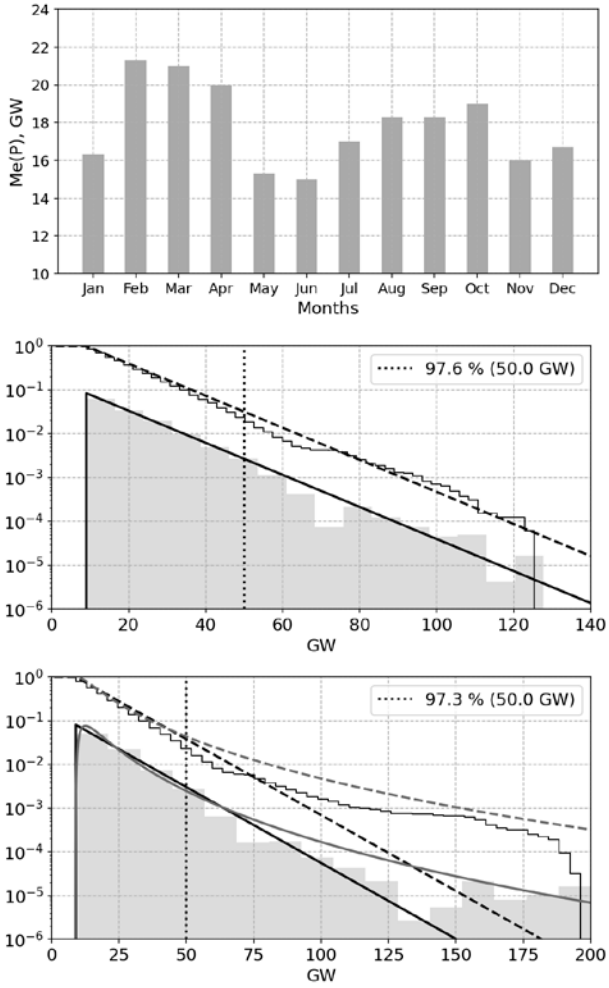

Figure 2. Monthly median values of aurora intensity generated by the computer model for the Northern Hemisphere (*a*); statistics of the forecast of integrated P_A for the Northern Hemisphere for November 2020 — October 2021 (*b*). Solid black and dashed lines denote probability density functions (*PDF*) and the survival function of the exponential distribution law. The thin black line indicates the empirical survival function; statistics of the forecast of integrated P_A for the Northern Hemisphere for 2021 (gray and black lines correspond to the lognormal and exponential distribution laws respectively (*c*))

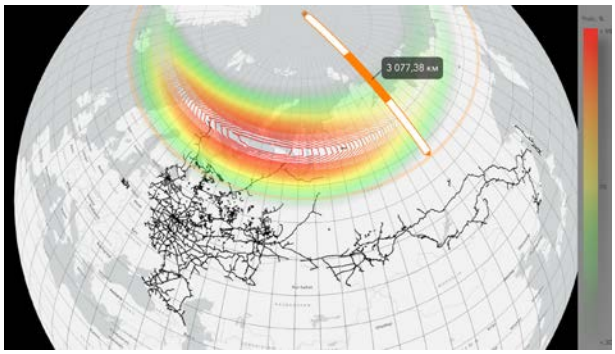

Figure 3. Result of simulation of spatial distribution of p_A

is at least ~60 %; yellow-orange, at least ~ 85 %; orange-red, at least 99 %. Northern track lines of the Oktyabrskaya (Murmansk—Moscow) and Northern (Yaroslavl—Arkhangelsk, Vologda—Vorkuta) railways are seen to be in the zone of intense auroras and current systems of the auroral oval even during moderate substorms. Intense geo-induced currents (GIC) and electric telluric fields can cause disruptions to signaling track circuits in these railway sections [Kasinsky et al., 2007; Boteler, 2021].

Thus, the proposed computer interactive model for short-term (30–70 min) forecast of spatial distribution of the probability of observing auroras can support management decisions aimed at reducing the risks of failure or breakdown in a number of technical systems of high-latitude infrastructure during periods of extreme geomagnetic activity.

In the near future, it is planned to implement support for thematic user layers including main power transmission lines. It is well known that high-latitude power transmission lines (for example, the 330 kV Kola-Karelian Transit) are affected by space weather [Vorobev et al., 2022]. The geoinformation system showing the relative position of the power transmission line networks and the predicted auroral oval will enable network operators to control the load in order to avoid failures (up to destruction) of substation power transformers [Vakhnina et al., 2018].

CONCLUSION

A multi-user computer model for short-term (with a horizon 30–70 min depending on the solar wind velocity) forecast of the intensity and spatial distribution of auroras has been developed. Verification of the forecast results, performed by comparing the simulation results with the data from all-sky cameras observing auroras in real time, has confirmed the adequacy of the model. The proportion of the confirmed forecast of auroras is more than 86 %, the proportion of type I and II errors is 14 and 26 % respectively.

Statistical analysis of the forecast of visibility of auroras, made with the OP model, has shown that for solar minimum the annual average probability of observing auroras in the visible spectrum $\left(P_A^N \geq 50\ \text{ГВт}\right)$ can be estimated as ~2.4 %, with the probability of observing extreme auroras $\left(P_A^N \geq 100\ \text{ГВт}\right)$ being ~ 0.1 %.

We have supported thematic user layers (the network of high-latitude railways, and main transmission lines in the near future), which can enable management decisions aimed at reducing the risk of failures of technical systems of high-latitude infrastructure during periods of extreme geomagnetic activity.

At present, the computer model formalized as a specialized web service is at the beta testing stage and is available at [http://aurora-forecast.ru]. According to monitoring data, the monthly average demand for the resource developed is ~1120 visits, which, given the specifics of the proposed service, indicates its relevance. Any suggestions for improving the web service will be gratefully accepted.

The study was financially supported by RSF (project No. 21-77-30010).

REFERENCES

Afraimovich E.L., Astafyeva E.I., Demyanov V.V., Gamayunov I.F. Mid-latitude amplitude scintillation of GPS signals and GPS performance slips. *Adv. Space Res.* 2009, vol.

43, pp. 964–972. DOI: 10.1016/j.asr.2008.09.015.

Boteler D.H. Modeling geomagnetic interference on railway signaling track circuits. *Space Weather*. 2021, no. 19. e2020SW002609. DOI: 10.1029/2020SW002609.

Demiyanov V.V., Yasukevich Yu.V. Space weather: risk factors for Global Navigation Satellite Systems. *Solar-Terr. Phys.* 2021, vol. 7, no. 2, pp. 28–47. DOI: 10.12737/stp72202104.

Hardy D.A., Holeman E.G., Burke W.J., Gentile L.C., Bounar K.H. Probability distributions of electron precipitation at high magnetic latitudes. *J. Geophys. Res.* 2008, vol. 113, A06305. DOI: 10.1029/2007JA012746.

Kasinsky V.V., Ptitsyna N.G., Lyakhov N.N., Tyasto M.I., Villoresi J., Jucci N. Influence of geomagnetic disturbances on the operation of railway automation and telemechanics systems. *Geomagnetizm i ajeronomiya* [Geomagnetism and Aeronomy]. 2007, vol. 47, no. 5, pp. 714–718. (In Russian).

Khorosheva O.V. *Prostranstvenno-vremennoe raspredelenie polyarnykh siyanii* [Spatial-temporal distribution of auroras]. Moscow: Nauka, 1967, 82 p. (In Russian).

Kosar B.C., MacDonald E.A., Case N.A., Zhang Y., Mitchell E.J., Viereck R. A case study comparing citizen science aurora data with global auroral boundaries derived from satellite imagery and empirical models. *J. Atmos. Solar-Terr. Phys.* 2018, vol. 177, pp. 274–282. DOI: 10.1016/j.jastp.2018.05.006.

Martines-Bedenko V.A., Pilipenko V.A., Hartinger M.D., Engebretson M.J., Lorentzen D.A., Willer A.N. Correspondence between the latitudinal ULF wave power distribution and auroral oval in conjugate ionospheres. *Sun and Geosphere*. 2018, vol. 13, no. 1, pp. 41–47.

Newell P.T., Sotirelis T., Wing S.J. Diffuse, monoenergetic, and broadband aurora: The global precipitation budget. *Geophys. Res.* 2009, no. 114, A09207. DOI: 10.1029/2009JA014326.

Newell P.T., Liou K., Zhang Y., Sotirelis T., Paxton L.J., Mitchell E. J. OVATION Prime-2013: Extension of auroral precipitation model to higher disturbance levels. *Space Weather*. 2014, no. 12, pp. 368–379. DOI: 10.1002/2014SW001056.

Penskikh Yu.V., Lunushkin S.B., Kapustin V.E. Geomagnetic method for automatic diagnostics of auroral oval boundaries in two hemispheres of Earth. *Solar-Terr. Phys*. 2021, vol. 7, no. 2, pp. 57–69. DOI: 10.12737/stp-72202106.

Pilipenko V.A. Space weather impact on ground-based technological systems. *Solar-Terr. Phys*. 2021, vol. 7, no. 3, pp. 68–104. DOI: 10.12737/stp-73202106.

Ptitsyna N.G., Tyasto M.I., Kasinsky V.V., Lyakhov N.N. Influence of space weather on technical systems: failures of railway equipment during geomagnetic storms. *Solnechno-zemnaja fizika* [Solar-Terrestrial Physics]. 2008, iss. 12, vol. 2, p. 360–363. (In Russian).

Pulkkinen A., Lindahl S., Viljanen A., Pirjola R. Geomagnetic storm of 29–31 October 2003: Geomagnetically induced currents and their relation to problems in the Swedish high-voltage power transmission system. *Space Weather*. 2005, no. 12, S08C03. DOI: 10.1029/2004SW000123.

Rozenberg I.N., Gvishiani A.D., Soloviev A.A., Voronin V.A., Pilipenko V.A. Influence of space weather on the reliability of railway transport in the Arctic zone of Russia. *Zheleznodorozhny transport* [Railway Transport]. 2021, no. 12, pp. 48–54. (In Russian).

Sokolova O.N., Sakharov Ya.A., Gritsutenko S.S., Korovkin N.V. Algorithm for analyzing the stability of power systems to geomagnetic storms. *Izvestija Rossijskoj akademii nauk. Jenergetika* [Bulletin of the Russian Academy of Sciences: Energetics]. 2019, pp. 33–52. (In Russian). DOI: 10.1134/S000233101 9050145.

Vakhnina V.V., Kuvshinov A.A., Shapovalov V.A. *Mekhanizmy vozdeistviya kvazi-postoyannykh geoindutsirovannykh tokov na elektricheskie seti* [Mechanisms of the impact of quasi-permanent geoinduced currents on electrical networks]. Moscow, Infra-Engineering Publ., 2018. 256 p. (In Russian).

Vorobjev V.G., Yagodkina O.I. Effect of magnetic activity on the global distribution of auroral precipitation zone. *Geomagnetism and Aeronomy*. 2005, vol. 45, no. 4, pp. 438–444.

Vorobev A.V., Pilipenko V.A., Enikeev T.A., Vorobeva G.R. Geoinformation system for analyzing the dynamics of extreme geomagnetic disturbances based on observation data from ground stations. *Kompyuternaya optika* [Computer Optics]. 2020a, vol. 44, iss. 5, pp. 782–790. (In Russian). DOI: 10.18287/2412-6179-CO-707.

Vorobev A.V., Pilipenko V.A., Krasnoperov R.I., Vorobeva G.R., Lorentzen D.A. Short-term forecast of the auroral oval position on the basis of the “virtual globe” technology. *Russ. J. Earth Sci*. 2020b, no. 20, p. ES6001. DOI: 10.2205/2020ES000721.

Vorobev A.V., Pilipenko V.A., Enikeev T.A., Vorobeva G.R., Khristodulo O.I. System for dynamic visualization of geomagnetic disturbances based on data from ground-based magnetic stations. *Nauchnaya vizualizatsiya* [Scientific Visualization]. 2021, no. 13.1, pp. 162–176. (In Russian). DOI: 10.26583/sv.13.1.11.

Vorobev A., Soloviev A., Pilipenko V., Vorobeva G., Sakharov Y. An approach to diagnostics of geomagnetically induced currents based on ground magnetometers data. *Applied Sciences*. 2022, no. 12, p. 1522. DOI: 10.3390/app12031522.

Yasyukevich Y., Vasilyev R., Ratovsky K. Small-Scale Ionospheric Irregularities of Auroral Origin at Mid-latitudes during the 22 June 2015 Magnetic Storm and Their Effect on GPS Positioning. *Remote Sens*. 2020, vol. 12, no 10, p. 1579. DOI: 10.3390/rs12101579.

Zakharov V.I., Chernyshov A.A., Miloh V., Jin Ya. Influence of the ionosphere on the parameters of the GPS navigation signals during a geomagnetic substorm. *Geomagnetism and Aeronomy*. 2020, vol. 60, no. 6, pp. 754–767. DOI: 10.1134/S0016793220060158.

URL: https://www.swpc.noaa.gov/products/aurora-30-minute-forecast (accessed October 4, 2022).

URL: https://en.vedur.is/weather/forecasts/aurora (accessed October 4, 2022).

URL: https://www.gi.alaska.edu/monitors/aurora-forecast (accessed October 4, 2022).

URL: https://github.com/lkilcommons/OvationPyme (accessed October 4, 2022).

URL: https://www.swpc.noaa.gov (accessed October 4, 2022).

URL: https://omniweb.gsfc.nasa.gov (accessed October 4, 2022).

URL: https://developers.arcgis.com/javascript/3 (accessed October 4, 2022).

URL: http://aurora-forecast.ru (accessed October 4, 2022).

This paper is based on material presented at the 17th Annual Conference on Plasma Physics in the Solar System, February 7–11, 2022, IKI RAS, Moscow.

Original Russian version: A.V. Vorobev, A.A. Soloviev, V.A. Pilipenko, G.R. Vorobeva, published in Solnechno-zemnaya fizika. 2022. Vol. 8. Iss. 2. P. 93–100. DOI: 10.12737/szf-82202213. © 2022 INFRA-M Academic Publishing House (Nauchno-Izdatelskii Tsentr INFRA-M)

How to cite this article

Vorobev A.V., Soloviev A.A., Pilipenko V.A., Vorobeva G.R. Interactive computer model for aurora forecast and analysis. *Solar-Terrestrial Physics*. 2022. Vol. 8. Iss. 2. P. 84–90. DOI: 10.12737/stp-82202213.